Waterspout Wind, Temperature and Pressure Structure Deduced from Aircraft Measurements

VERNE H. LEVERSON AND PETER C. SINCLAIR

Department of Atmospheric Science, Colorado State University, Fort Collins 80523

JOSEPH H. GOLDEN[1]

Environmental Research Laboratories, NOAA, Boulder, Colo. 80302

(Manuscript received 13 August 1976, in revised form 28 February 1977)

ABSTRACT

During September 1974 in the Lower Florida Keys, the first successful penetrations of mature waterspouts were accomplished by a specially instrumented research aircraft. Throughout the course of each penetration, the measurement system recorded the temperature, the pressure and the three-dimensional velocity field near and within the visible funnel. Multiple penetrations of both cyclonic and anticyclonic waterspouts in various life-cycle stages were achieved. The results indicate that the waterspout funnel structure exhibits 1) a warm central core region, 2) positive vertical velocities of 5–10 m s^{-1} outside of the warm core, and 3) tangential velocities and horizontal pressure gradients with characteristics similar to but with magnitudes greater than those of the dust devil. A scale analysis of each term in the governing equations of motion suggests a simplified set of modeling equations. The simple Rankine-combined vortex model with cyclostrophic flow explains approximately 75% of the total measured pressure deficit. This compares favorably with Sinclair's (1966, 1973) earlier results for the dust devil vortex.

1. Introduction

The tornado continues to be one of the most enigmatic and elusive meteorological phenomena to understand. Every year, especially during the spring and summer months, the entire United States east of the Rockies is susceptible to the onslaught of tornadoes. Davies-Jones and Kessler (1974) reported that from 1953–72 an average of 113 persons were killed annually by tornadoes with a corresponding average annual property loss of $75 million. During the same period, only lightning caused a higher average annual number of human fatalities from severe storms. The worst tornado outbreak to affect the United States in recorded history occurred on 3–4 April 1974. Though well forecast, 148 tornadoes were responsible for over 300 deaths in about a 16 h period (Fujita, 1976). The continued urbanization of large parts of the United States increases the risk of tornado devastation in those areas each year. Furthermore, it must be recognized that our basic understanding of tornado structure and behavior is not complete; improvement in this understanding requires among other things more direct tornado observations.

The only direct quantitative assessments of tornado flow fields to date have been obtained by photogrammetric analysis of fortuitous eyewitness and news-media photography of tornadoes (Hoecker, 1960; Fujita, 1976; Agee *et al.*, 1975). Subsequent analyses of tornado damage and debris configurations on the ground (e.g., cycloidal suction swaths) have yielded useful but sometimes conflicting surface wind speed estimates (Fujita, 1970; Mehta *et al.*, 1971). The pressure and temperature profiles through tornadoes remain virtually unknown. Some success at purposefully intercepting, tracking and photographing tornadoes and their attendant cloud structures from a radio-equipped van on the ground has been reported (Golden and Morgan, 1972). Rotational and vertical flow components have been photogrammetrically derived in the debris and cloud-tags around a large tornado intercepted in Oklahoma (Golden and Purcell, 1974).

Because of the lack of accurate and sufficient tornado measurements, relatively slow progress has been made in numerical and laboratory modeling of small-scale convective vortices which have tornado-like features (e.g., Gutman, 1957; Kuo, 1966, 1969; Leslie, 1971; Ying and Chang, 1970; Ward, 1972). However, our analyses and those of others (Lilly, 1965) indicate that some of the assumptions inherent in these and other modeling attempts remain open to doubt until they can be checked with more quantitative observational data.

Improved understanding of tornado structure will not be forthcoming until we obtain much better mea-

[1] Research completed while this author was associated with National Severe Storms Laboratory, NOAA, Norman, Okla. 73069.

FIG 1. Subcloud severe storms measurement aircraft. The North American T-6 aircraft has been extensively modified to carry the AADS-2B system. The boom structure positions some of the sensing probes ahead of the aircraft to minimize fuselage-wing flow and pressure effects. The boom supports the Rosemount temperature sensor, pitot-static tube and the α, β vane system. The α and β vane units, along with the gyro-referenced platform, provide data on the vertical and lateral air motions near and within the severe storms. The vanes are constructed of lightweight balsawood and are internally mass balanced to improve the response characteristics. The boom is of aluminum-stainless steel construction and has a natural frequency of 11 Hz.

surements of the vortex wind, pressure and temperature fields. Because of the intensity and relatively short duration of the tornado vortex we do not have adequate instrumentation to accomplish the necessary observations. In order to guide us in the development of these observational systems and techniques, we have been studying a close relative to the tornado—the waterspout.[2] Golden (1974a,b) has given evidence which indicates strongly that waterspouts and tornadoes are qualitatively the same, but differ in only certain quantitative characteristics. These differences encompass vortex size and intensity, structure of the mesoscale environment, and intensity and organization of the parent convection. Preliminary measurements by Golden (1974a,b) and Church *et al.* (1973) have indicated from observations in Key West, Fla., where waterspouts frequently occur (Golden, 1970), that waterspout horizontal winds above the spray vortex maximum are approximately 25–35 m s^{-1} and the funnel core is slightly warmer than the environment.

The purpose of this paper is to provide some new data and insights on the distribution of wind, pressure and temperature near and within the waterspout funnel. The measurements are considered to be the first obtained by the direct penetration of the visible funnel with an instrumented research aircraft. The aircraft measurement system (Sinclair, 1973a, 1974b) was developed by the Severe Storm Measurement and Analysis Group (SSMAG) of the Atmospheric Science Department, Colorado State University (CSU). During the period 15–27 September 1974 the aircraft system was deployed to Key West. During this period, 16 waterspout funnels were penetrated up to 17 successive times each.

[2] We define the waterspout as an intense columnar vortex (usually containing a funnel cloud) of small horizontal extent which occurs over a body of water (Golden, 1971).

2. Airborne measurement technique

a. System requirements

In order to formulate a waterspout model which is physically more realistic than, for example, Gutman's (1957) numerical model, a measurement program of considerable detail as well as scope is required. Initially, this measurement program has been based primarily on the direct probing of the waterspout funnel, the parent cloud and the immediate environment of the funnel-cloud system. This requires the use of sophisticated airborne systems that are capable of accurately measuring physical and kinematic variables across and within the boundaries of the waterspout funnel. In addition, it is mandatory that measurements be made at several levels within the waterspout-cloud system and the environment in a systematic manner that permits optimum space-time interpretation of the data.

In addition to the multiple-level sampling requirements of the airborne platform, the measurement systems should be capable of recording the temperature, pressure, moisture, liquid water content and the three-dimensional velocity and turbulence structure of both the environment and the waterspout funnel-cloud system. The accuracy and space resolution of these measurements must be such that they are compatible with modeling requirements and possible cloud modification design requirements. For example, our past experience in cumulus-type cloud penetration measurements and modeling requirements indicates that the waterspout funnel-cloud system will probably require temperature and air velocity measurement accuracies of at least ± 0.1°C and ± 0.5 m s^{-1}, respectively. Also, adequate space resolution of data collected from an aircraft platform near and within the waterspout funnel requires instrument response times of 0.1 s. This virtually eliminates the use of the aircraft itself as part of the measurement system in the sensing of the wind velocity components in these regions of the waterspout.

b. System design

Over the past five years, several airborne measurement systems have been developed by SSMAG at Colorado State University. These systems have been or are presently being used to measure the three-dimensional velocity, temperature, pressure and humidity fields near and within severe storms. The

technology and some of the hardware of three Airborne Atmospheric Data Systems (AADS) [the North American T-6/T-28 AADS-2B, the Canadair T-33, AADS-3B (Sinclair 1969b) and the F-101B, AADS-4A (Sinclair, 1973a)] have been utilized in developing the waterspout project airborne measurement system. The AADS-2B (Fig. 1) in its present configuration is capable of obtaining direct measurements of the three-dimensional velocity field, temperature and pressure near and within the waterspout-cloud system. The measurement system is designed so as to be independent of the aircraft sensitivity to atmospheric motions and/or pilot-induced motions. The measurement technique (Sinclair, 1969b) requires knowledge of the motion of the air relative to the airplane ($V_{a,p}$) and the motion of the airplane relative to the ground ($V_{p,g}$) in order to calculate the atmospheric motion with respect to the ground ($V_{a,g}$); thus

$$\mathbf{V}_{a,g}=\mathbf{V}_{a,p}+\mathbf{V}_{p,g},$$

which for the vertical component ($w_{a,g}$) can be expressed as

$$w_{a,g}=V_T\alpha+V_T\beta\phi-V_T\theta+\int_0^t a_z dt+w_{p,g}(0)+L\dot{\theta},$$

where V_T is the true airspeed; α the angle of attack; θ, β and ϕ the pitch, yaw and roll angles, respectively; a_z the vertical acceleration of the aircraft; $w_{p,g}(0)$ the vertical motion of the aircraft at time $t=0$; $\dot{\theta}$ the pitch rate; and L the accelerometer displacement from the angle of attack measurement point. The measurement of α and β are made with lightweight, but durable, flow vanes. The aircraft pitch and roll angles and the pitch rate (ϕ) are measured with high precision vertical and rate gyros. Accelerations are measured by a three-axis accelerometer system at the aircraft center of gravity and the true airspeed is calculated from measurements of total ram and static pressures. Relatively fine structure of the turbulent velocity spectrum (0.04–10 Hz) can be obtained from the data which are recorded on a 1000 character per second, digital, incremental magnetic tape recorder. The AADS-2B permits detailed measurements of the visible funnel structure. That is, approximately 15–30 data points of all parameters are recorded for an average funnel diameter of 25 m. All funnel penetrations are made with a minimum of aircraft control and power changes. Ideally, the approach to the visible funnel proceeds from an initial point ~0.5 km upwind to the funnel boundary in a constant altitude mode. The funnel penetration is made with essentially constant attitude fixed controls at a constant altitude. A similar 0.5 km downwind track is accomplished after funnel penetration. This procedure allows space-time referencing of the AADS-2B and detection of the wind, pressure and temperature fields surrounding the visible funnel. The idealized flight track, however, must usually be modified to accomodate cloud and precipitation development.

Most of the AADS-2B system is mounted below the right wing of the T-6 aircraft in a modified T-33 drop tank (Fig. 1). The α, β vane system and pitot tube are mounted at the front of the instrumentation boom which extends from the nose of the drop tank to a point ahead of the plane of the propellor. Since vertical accelerations of the aircraft may range from ± 1–$3g$ incremental, it is imperative that only certain (many are negative g-limited) military stressed aircraft are used in and near the waterspout funnel. In addition, the aircraft must be fully aerobatic in order to recover easily from all possible attitudes. All commercial aircraft fail to meet either these airframe and maneuverability requirements or the instrumentation load capacity and low speed requirements, or both. These safety requirements and performance capabilities, while well-recognized by aircraft oriented organizations, have not always been appreciated by atmospheric research groups (RAND, 1968). We consider this type of system a necessary requirement for obtaining accurate pressure, temperature and wind measurements in the waterspout environment.

3. Penetration case studies

During the 12-day period from 16 September–27 September 1974, a total of 16 waterspouts were penetrated by the instrumented aircraft. The life-cycle stages of the penetrated waterspouts included all of Golden's (1974a,b,c) five documented stages except the spiral stage. Multiple penetrations were made on 7 of the 16 waterspouts, and in one case two cyclonic waterspouts were penetrated 26 successive times with no apparent effect on the vortex structure. The majority of the waterspouts ranged from weak to moderate in intensity, i.e., maximum upward vertical velocities <10 m s^{-1} and maximum tangential velocities <30 m s^{-1} at penetration attitudes of >400 m MSL.

In this section, three representative penetrations are presented in terms of horizontal profiles of vertical velocity, horizontal velocity, temperature and core pressure deficit. All velocities are measured relative to a cylindrical coordinate system fixed to and moving with the waterspout. The measurement technique has been designed such that the aircraft penetration track and the boom-vane system longitudinal axis pass through the spout center along the radial coordinate. That is, only the radial velocity component requires significant correction due to the combined motion of the waterspout and the aircraft. As a result, the transverse horizontal velocity v presented in this paper represents the waterspout's tangential velocity.

a. Cylonic waterspout

The first cyclonic waterspout was one of two adjacent cases documented at midday on 20 September. Both

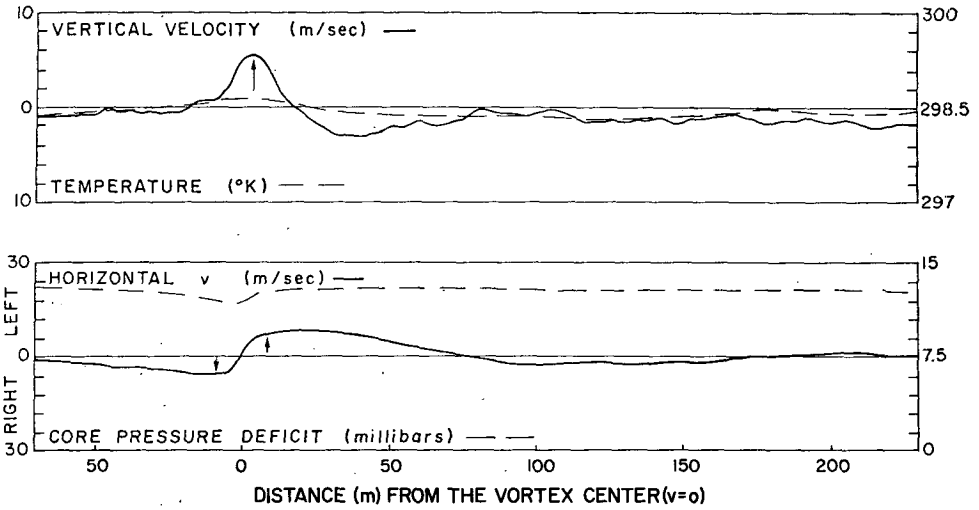

FIG. 2. Profiles of vertical velocity, horizontal velocity, temperature and pressure for a cyclonic waterspout along the penetration flight path. Horizontal velocities are directed to the left or right of the aircraft's direction of flight. Pressure is the deviation from an environmental reference pressure far from the funnel. The cyclonic waterspout occurred 20 September 1974. Penetration altitude was approximately 490 m, and the funnel diameter at the time of penetration was approximately 10–14 m.

spouts existed at the dark spot stage (Golden, 1973a) with funnel clouds extending down from cloud base approximately 100–150 m. The two waterspouts did not form simultaneously; the second was initially sighted approximately 16 min into the first waterspout's total lifetime of 23 min. The demise of the second spout occurred approximately 6 min after the first vortex decay.

Fig. 2 illustrates the horizontal profiles of vertical velocity, tangential velocity, temperature and core pressure deficit through the visible funnel. Each trace encompasses 5 s of data sampling.

The vertical velocity trace shows a singular, broad, quasi-symmetric peak of upward motion existing in the funnel, with maximum values of 5.8 m s^{-1}. A 2.9 m s^{-1} downdraft immediately behind the funnel rapidly ($\sim$1 s) approaches the near-waterspout environmental value of approximately -1 m s^{-1}. During the next 8 s of flight (not shown), the vertical velocity approaches zero before the aircraft penetrates the second waterspout.

The cyclonic flow of the waterspout is clearly shown in the tangential wind velocity profile[3] (Fig. 2). A broad circulation is evident, with the wind velocities decreasing slowly outward from the radius of maximum winds. Slight asymmetry in the v profile exists because v_{max} on the front and back sides (with respect to the penetration) of the waterspout is 5.4 and 8.5 m s^{-1}, respectively.

The temperature structure of the waterspout exhibits a positive anomaly of $\sim$0.3 K that coincides with the maximum updraft velocities. This increase in temperature is similar to that found in dust devils (Sinclair 1966, 1973b) and results from the upward transport of warmer air from lower levels. Differing only in magnitude, this temperature profile, with a single positive peak, is similar to most other waterspouts penetrated.

The maximum core pressure deficit of $\sim$1.3 mb coincides with the defined vortex center of $v=0$. Slightly less coincidence is shown between the minimum core pressure and the maximum positive values of temperature and vertical motion. These preliminary results, as well as the succeeding examples, show for the first time from direct measurements that the waterspout structure can be characterized by a warm, low-pressure vortex. This structure is very similar to that found by Sinclair (1966, 1973b, 1974a) for the upper levels of desert dust devils. Thus, two geophysical vortices formed by quite different initiating mechanisms exhibit similar structual characteristics. We suspect that comparable *in-situ* measurements near and within the tornado funnel will also show a warm, low-pressure vortex.

b. Intensifying anticyclonic waterspouts

The first of two penetrations through an anticyclonic waterspout is shown in Fig. 3. Again, only 5 s of data sampling is given in order to more clearly show the symmetry and coincidence of the temperature, pressure and wind profiles near and within the visible vortex. This waterspout was not penetrated until it had reached the spray vortex stage of its life cycle with a fully extended funnel from cloud base to sea surface. A second waterspout was penetrated after the one shown in Fig. 3, but it was significantly weaker and

[3] Note that all wind velocities are to be considered relative winds with respect to the vortex center, and that reference to front (forward) and near (back) sides of the waterspout is with respect to the aircraft penetration track.

was engulfed by a moderate rain shower after one penetration. The stronger waterspout (Fig. 3) lasted approximately 7 min after the first sighting. During the decay stage of the vortex, the rain shower almost completely wrapped around the funnel, and the upper one-third of the funnel was tilted about 60° from the vertical.

The vertical velocity profile shows an ambient, near-waterspout value of $\sim$1.5 m s^{-1}. This rising motion increases gradually (in $\sim$0.7 s) to a maximum of 6.8 m s^{-1} near the apparent waterspout center. Immediately after penetration an abrupt downdraft of 4.9 m s^{-1} was encountered. The remainder of the trace shows a return to the ambient upward vertical motions characteristic of the waterspout-cloud base environment. The weak subsidence in the funnel core inferred from previous observations (Golden, 1971, 1973a) may have been smoothed out because of small waterspout sizes and penetration speeds.

The waterspout's tangential wind velocity (v) field is marked by broad-scale circulation characteristics and slight asymmetry. The maximum values of v are 5.2 m s^{-1} on the forward side and 9.3 m s^{-1} on the rear of the waterspout.

The temperature and core pressure deficit traces exhibit maximum anomalies of +0.3 K and −3.2 mb, respectively. These values occur almost simultaneously with the maximum vertical velocity and lie approximately midway between the two v maxima.

c. *Mature anticyclonic waterspout*

The profiles in Fig. 4 are the results of a penetration of the same anticyclonic waterspout 1.5 min after the penetration shown in Fig. 3. In that amount of time the waterspout parameters have markedly intensified. This intensification can be due to either a strengthening of the mature vortex prior to decay or to an off-center penetration of the funnel during the first penetration (Fig. 3). The latter possibility would have reduced the magnitude of variation of all measured variables (except u) below that of the core values.

The vertical velocity trace shows a characteristic 1–2 m s^{-1} value in the near-waterspout environment prior to penetration. As the boom-vane system on the aircraft (Fig. 1) penetrates the spout, there is a rapid, almost instantaneous, increase in the vertical motion to a maximum value of $\sim$ 8 m s^{-1}. From this maximum, the vertical velocity decreases much more slowly to the rear of the funnel. A distinct downdraft of $\sim$3.5 m s^{-1} was again encountered on the backside following the penetration, in a region of developing heavy rain-showers.

The tangential wind velocities measured during this penetration were the strongest recorded during the 12-day program. The maximum values for v were 13.1 and 28.1 m s^{-1} for the front and back sides of the spout, respectively. Once again, asymmetry of the clockwise circulation is apparent. This asymmetric flow that has appeared in each of the presented cases appears to be due to one or both of the following factors: 1) neglect of the yaw accelerations of the aircraft during the penetrations, and 2) the slope of the waterspout funnel with respect to the aircraft penetration heading. Preliminary integration of the aircraft yaw accelerations has shown that a significant reduction in the measured asymmetry of the tangential wind profiles can be accomplished. It is anticipated that funnel slope corrections will also yield similar results. These corrections will be incorporated in a more detailed paper at a later date. However, taking into account the asymmetry of the flow, the tangential

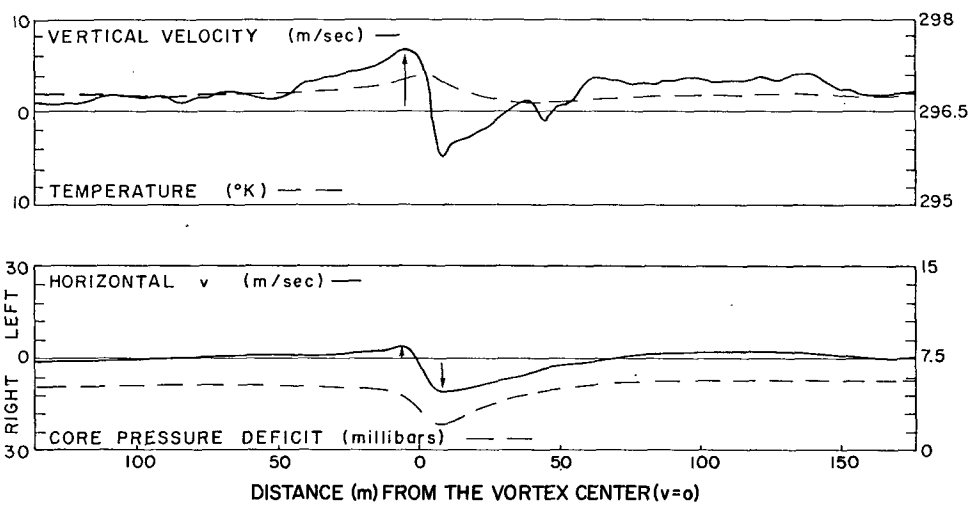

FIG. 3. As in Fig. 2 except for an intensifying anticyclonic waterspout. The anticyclonic waterspout occurred 20 September 1974. Penetration altitude was approximately 670 m and the funnel diameter at the time of penetration was approximately 15–20 m.

wind data indicate that the waterspout vortex closely approximates a Rankine-combined vortex. This will be further discussed in a following section.

The waterspout's temperature exhibits a sinusoidal variation with a positive core anomaly of 0.2 K that drops ~0.5 K to a minimum on the back side of the funnel. This profile differs from our other penetration data. Several explanations may be responsible for rapid cooling outside of the funnel, i.e., a slightly wet sensor, evaporative cooling, or vortex entrainment of cooler air from the rain shower within 3–4 funnel diameters of the visible spout.

The core pressure deficit shows an abrupt drop of 8.5 mb in pressure from the environment to the center of the funnel with a less rapid recovery on the back side of the funnel. This core of minimum pressure demonstrates good spatial correlation with the temperature maximum, the waterspout center where $v=0$, and the beginning of the rapid vertical velocity rise. The maximum values of v occur at 4–5 mb below the reference pressure, i.e., in the region of large $\partial p/\partial r$.

4. Scale analysis

To facilitate a quantitative description and to help formulate a model of the waterspout dynamic characteristics, the equations of motion have been reduced to a simplified set by a scale or order-of-magnitude analysis of each term. Characteristic magnitudes are obtained as representative values from the three case studies presented. The three scalar components of the vector equation of motion for steady-state, incompressible flow with constant eddy viscosity in cylindrical coordinates may be written

$$u\frac{\partial u}{\partial r}+\frac{v}{r}\frac{\partial u}{\partial \theta}+w\frac{\partial u}{\partial z}-\frac{v^2}{r}=-\frac{1}{\rho}\frac{\partial p}{\partial r}+K\left[\frac{\partial^2 u}{\partial r^2}+\frac{1}{r}\frac{\partial u}{\partial r}+\frac{1}{r^2}\frac{\partial^2 u}{\partial \theta^2}+\frac{\partial^2 u}{\partial z^2}\right], \quad (1)$$

$$u\frac{\partial v}{\partial r}+\frac{v}{r}\frac{\partial v}{\partial \theta}+w\frac{\partial v}{\partial z}+\frac{uv}{r}=-\frac{1}{\rho r}\frac{\partial p}{\partial \theta}+K\left[\frac{\partial^2 v}{\partial r^2}+\frac{2}{r}\frac{\partial v}{\partial r}+\frac{1}{r^2}\frac{\partial^2 v}{\partial \theta^2}+\frac{\partial^2 v}{\partial z^2}\right], \quad (2)$$

$$u\frac{\partial w}{\partial r}+\frac{v}{r}\frac{\partial w}{\partial \theta}+w\frac{\partial w}{\partial z}=-\frac{1}{\rho}\frac{\partial p}{\partial z}-g+K\left[\frac{\partial^2 w}{\partial r^2}+\frac{1}{r}\frac{\partial w}{\partial r}+\frac{1}{r^2}\frac{\partial^2 w}{\partial \theta^2}+\frac{\partial^2 w}{\partial z^2}\right], \quad (3)$$

where u, v, w are the mean wind components in the r, θ, z directions, respectively, p is the mean pressure, ρ the mean ambient air density, g the acceleration of gravity, and K a constant coefficient of eddy viscosity. Note also that the Coriolis acceleration terms are omitted since for small vortices such as waterspouts, dust devils, etc., they are known to be several orders of magnitude smaller than the remaining terms (Sinclair, 1966, 1969a).

Characteristic values for the components of the three-dimensional wind field are chosen from the strongest case presented in this paper, that shown in Fig. 4. This is done so as to represent realistic values of a moderately intense waterspout. The characteristic values selected are $v=25$ m s^{-1}, $w=8$ m s^{-1} and $u=1$ m s^{-1}. The value of u is based upon estimates from a large waterspout made by Golden (1974a) and applied to this somewhat weaker case. We take $r=40$ m, where r is the vortex scale radius (not necessarily the visible funnel), and $z\approx 40$ m, where z is the vertical distance between two successive funnel penetrations. These values are chosen from visual observations and the reduced data. Finally, a core pressure deficit Δp of 8.5 mb is selected.

In applying these characteristic values to each term of the r equation of motion, the inertial term for the centripetal acceleration (v^2/r) and the radial pressure gradient term are at least three orders of magnitude larger than the next largest term. Therefore, the r equation of motion can be approximated by $v^2/r=-\rho^{-1}\times(\partial p/\partial r)$ which is simply the cyclostrophic wind relation. This same reduction of the r equation has also been accomplished by Golden (1974a) from analysis of photographic data of the waterspout funnel and spray vortex. Sinclair (1966) has also shown for the dust devil vortex near the ground that the cyclostrophic relation accounts for most of the balance within the r equation (disregarding friction). While the assumption of cyclostrophic motion does give a fair estimate of the radial pressure distribution, and hence may be helpful in deducing total pressure drops in violent systems such as the tornado, the departure from cyclostrophic "balance" is in essence the basic feature of the waterspout and dust devil vortex flow. Consequently, other terms in the r equation must be retained in order to adequately describe and model these flow fields.

Assuming axial symmetry in the wind and pressure fields, the θ equation can be used to obtain an approximate mean value for K. A scale analysis of the three inertial terms and the three eddy viscosity terms indicates that $K\approx 40$ m^2 s^{-1}. This compares favorably with the value $K\approx 100$ m^2 s^{-1} found by Golden (1974a) for waterspouts and Sinclair's (1966) values of $K=5$–15 m^2 s^{-1} for dust devils.

The vertical component of the equation of motion after scale analysis shows that the pressure gradient term is of the same order of magnitude as the acceleration of gravity, i.e., the vertical flow field is approximately in hydrostatic balance. However, the departures from hydrostatic balance produce many important waterspout features. If the terms with the largest

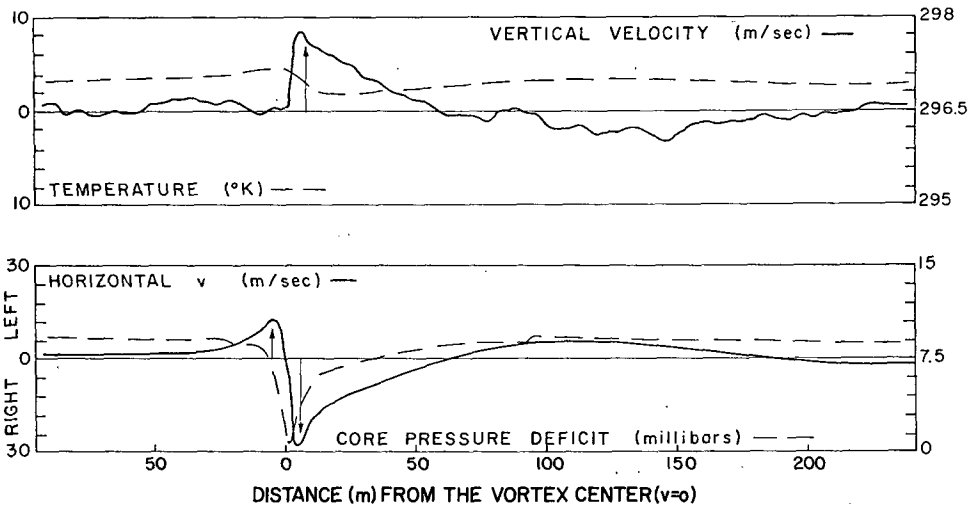

FIG. 4. As in Fig. 3 except for a mature anticyclonic waterspout. Penetration altitude was approximately 645 m and the funnel diameter at the time of penetration was approximately 15–20 m.

order of magnitude (shown in brackets below each term) are retained, the equation can be written

$$\underset{[0.1]}{u\frac{\partial w}{\partial r}}+\underset{[0.1]}{w\frac{\partial w}{\partial z}}=\underset{[10]}{-\frac{1}{\rho}\frac{\partial p}{\partial z}}\underset{[10]}{-g}+\underset{[0.1]}{K\frac{\partial^2 w}{\partial r^2}}+\underset{[0.1]}{K\frac{1}{r}\frac{\partial w}{\partial r}}. \quad (4)$$

Whether the two inertial terms may be appreciable remains to be investigated from a more detailed analysis of successive, multi-level funnel penetrations. A more detailed analysis is now being conducted in order to ascertain the importance of each term as a function of the radial and vertical coordinates. This will reveal the regions near and within the waterspout circulation where each term has significant importance.

5. Rankine-combined vortex

To obtain some idea of how well the waterspout measurements may be explained by a simple model, consider a steady circular vortex (cyclostrophic motion) with the tangential velocity described by a Rankine vortex, i.e., solid rotation in the core and irrotational motion outside of the core. Fig. 5 illustrates the closeness with which the Rankine vortex fits the tangential wind velocity trace of the mature anticyclonic waterspout (Section 3c). Adjusting for the asymmetric flow, the fit chosen seems to best represent the data. From the vortex core, where $v=0$, to the radius of maximum tangential winds, where $v=25$ m s^{-1}, the Rankine vortex exhibits a flow field in solid rotation, i.e., the tangential velocity is directly proportional to the radius of $v=c_1 r$. Outside the radius of maximum winds, the v field is one of irrotational motion or $v=c_2 r^{-1}$ (c_1 and c_2 are constants). The tangential field of motion closely approximates the $v=c_2 r^{-1}$ relationship on the front side of the funnel and $v=c_2 r$ relationship through the waterspout core. On the back side, however, the velocity trace beyond $v_{max}=28$ m s^{-1} departs markedly from the Rankine model, i.e., the v measurements more closely approach that of a $v=c_3 r^{-\frac{1}{2}}$ profile until an approximate value of 10 m s^{-1} is reached ($r\approx 28$ m). From this radius, v decreases linearly to zero at ~ 58 m.

The scale analysis of the r equation of motion indicates that the cyclostrophic relation is a valid first approximation for describing the tangential flow field in the upper levels of the waterspout funnel. If we use the Rankine-combined vortex to describe the tangential wind distribution, the cyclostrophic relation requires a total presure deficit of 6.23 mb. The measured waterspout pressure deficit was 8.50 mb. The simple cyclostrophic-Rankine-combined vortex model is thus capable of explaining approximately 75% of the total measured pressure deficit. This compares very favorably with Sinclair's (1966, 1973b) dust devil measurements which showed that this same simple model was capable of explaining approximately 75% of the total mean pressure drop from the environment to the dust devil center. With respect to the waterspout and the dust devil results, the discrepancy between the measured pressure deficit and that calculated from the simple cyclostrophic vortex model is attributed to the neglect of radial inflow and vertical motion in the model. Since radial inflow and vertical motion are characteristic of the waterspout structure at all altitudes, calculations of a core pressure deficit from the tangential wind field alone will obviously be less than the true value. In this case, inaccuracies based on the somewhat arbitrary fitting of the Rankine vortex must also certainly exist. Also, terms in the r equation of motion containing u may be of larger magnitude than that analyzed, particularly the inertial and turbulence terms containing $\partial u/\partial z$.

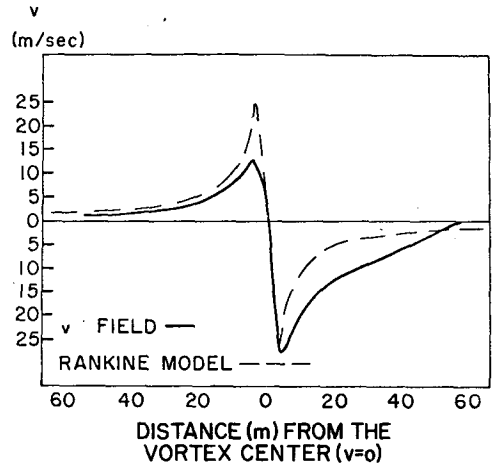

FIG. 5. Rankine model fit to the horizontal velocity profile of Fig. 4.

6. Conclusions

The waterspout velocity, temperature and pressure fields obtained by an airborne measurement system have been presented and examined to produce an integrated picture of the waterspout vortex structure in the near-cloud base environment. The data show that in the waterspout funnel there exist 1) a core of rising motion of 5–10 m s^{-1}, 2) a horizontal circular flow field that is broader in weaker waterspouts and spatially concentrated in more intense waterspouts, 3) a central core region $\sim$0.3 K warmer than the environment, and 4) a core pressure deficit on the order of $\sim$1–10 mb depending on waterspout intensity. Based on these data, some simplifications to the cylindrical, incompressible equations of motion have been made by an order-of-magnitude scale analysis of each term. While the present form of the reduced equations represent only a rough approximation, it has been shown that the cyclostropic relation and a Rankine-combined vortex model account for a considerable portion of the measured total pressure deficit. A more detailed measurement program was conducted during the 1975 waterspout season in order to document more fully the dynamic structure of larger and more intense waterspouts. Hopefully, these studies will lead to a greater insight into the waterspout's more energetic relative, the tornado.

Acknowledgments. The authors express their appreciation to the National Oceanic and Atmospheric Administration for their support under Grant 04-5002-8 which made this work possible and to the Nuclear Regulatory Commission for partial support in the data analysis phase of the research. Also we extend our gratitude to Mr. George Faraldo, Airport Manager of Key West International Airport, and Mr. Richard Urbanak, Meteorologist-in-Charge of the Weather Service Office in Key West, for their assistance and cooperation during the field program. The capable maintenance and technical support of the aircraft and instrumentation systems during the field program by Messrs. Jerrell Wilkey and Donald Hill are gratefully appreciated. Also we wish to thank Messrs. Lyle Lilie and Thomas Grove for their expert assistance in preparation of the AADS-2B for the field program. Special thanks go to Mr. David Younkin, the reserach pilot, and Ms. Karen Greiner who typed the manuscript.

REFERENCES

Agee, E., C. Church, C. Morris and J. Snow, 1975: Some synoptic aspects and dynamic features of vortices associated with the tornado outbreak of 3 April 1974. *Mon. Wea. Rev.*, **103**, 318–333.

Church, C. R., C. M. Ehresman and J. H. Golden, 1973: Instrumentation for probing waterspouts. *Preprints Eight Conf. Severe Local Storms*, Denver, Colo., Amer. Meteor. Soc., 169–172.

Davies-Jones, R. P., and E. Kessler, 1974: Tornadoes. *Weather and Climate Modification*, W. N. Hess, Ed., Wiley, 842 pp. (see Chap. 16).

Fujita, T. T., 1970: The Lubbock tornadoes: A study of suction spots. *Weatherwise*, **23**, 160–173.

——, 1976: Graphic examples of tornadoes. *Bull. Amer. Meteor. Soc.*, **57**, 401–412.

Golden, J. H., 1970: The lower Florida Keys waterspout project, May–Sept., 1969. *Bull. Amer. Meteor. Soc.*, **51**, 235–236.

——, 1971: Waterspouts and tornadoes over South Florida. *Mon. Wea. Rev.*, **99**, 146–154.

——, 1973a: The life cycle of the Florida Keys waterspout as the result of five interacting scales of motion. Ph.D. dissertation, Florida State University, 371 pp.

——, 1973b: Some statistical aspects of waterspout formation. *Weatherwise*, **26**, 108–117.

——, 1974a: Life cycle of Florida Keys waterspout. NOAA Tech. Memo. ERL-NSSL-70, National Severe Storms Lab., 247 pp.

——, 1974b: The life cycle of Florida Keys waterspout, I. *J. Appl. Meteor.*, **13**, 676–692.

——, 1974c: Scale interaction implications for the waterspout life cycle. II. *J. Appl. Meteor.*, **13**, 693–709.

——, and B. J. Morgan, 1972: The NSSL-Notre Dame tornado intercept program, spring 1972. *Bull. Amer. Meteor. Soc.*, **53**, 1178–1180.

——, and D. Purcell, 1974: Velocity and morphological analysis of Union City, Oklahoma tornado, May 24, 1973. *Trans. Amer. Geophys. Union*, **56**, p. 1130 (abstract).

Gutman, L. N., 1957: Theoretical model of a waterspout. *Bull. Acad. Sci. USSR Geophys. Ser.*, **1**, 87–103.

Hoecker, W. H., 1960: Wind speed and air flow patterns in the Dallas tornado of April 2, 1957. *Mon. Wea. Rev.*, **88**, 167–180.

Kessler, E., 1970: Tornadoes. *Bull. Amer. Meteor. Soc.*, **51**, 966–936.

Kuo, H. L., 1966: On the dynamics of convective atmospheric vortices. *J. Atmos. Sci.*, **23**, 25–42.

——, 1969: Axially-symmetric flows in the boundary layer of a maintained vortex. Planetary Circulation Project, Rep. No. 15, Dept. Geophys. Sci., University of Chicago, 57 pp.

Leslie, L. M., 1971: The development of concentrated vortices: A numerical study. *J. Fluid Mech.*, **48**, 1–21.

Lilly, D. K., 1965: Experimental generation of convectively driven vortices. *Geofis. Intern.*, **5**, 43–48.

Mehta, K. C., J. R. McDonald, J. E. Minor and A. J. Sanger, 1971: Response of structural systems to the Lubbock storm. Storm Res. Rep. 03, Institute for Disaster Research, 428 pp.

RAND, 1968: Weather modification progress and the need for interactive research. Tenth Annual Report, NSF.

Sinclair, P. C., 1966: A quantitative analysis of the dust devil. Ph.D. dissertation, University of Arizona, 292 pp.

——, 1969a: General characteristics of dust devils. *J. Appl. Meteor.*, **8**, 32–45.

——, 1969b: Vertical motion and temperature structure of severe convective storms. *Preprints Sixth Conf. Several Local Storms*, Chicago, Ill., Amer. Meteor. Soc., 346–350.

——, 1973a: Severe storm air velocity and temperature structure deduced from penetrating aircraft. *Preprints Eighth Conf. Severe Local Storms*, Denver, Colo., Amer. Meteor. Soc., 25–32.

——, 1973b: The lower structure of dust devils. *J. Atmos. Sci.*, **30**, 1599–1619.

——, 1974a: Vertical transport of desert particulates by dust devils and clear thermals. *Proc. Atmosphere-Surface Exchange of Particulate and Gaseous Pollutants*, Richland, Wash., Atomic Energy Commission, 497–527.

——, 1974b: Severe storm turbulent energy structure. Preprints *Sixth Conf. Aerospace and Aeronautical Meteor.*, El Paso, Tex., Amer. Meteor. Soc., 36–39.

Ward, N. B., 1972: The exploration of certain features of tornado dynamics using a laboratory model. *J. Atmos. Sci.*, **29**, 1194–1204.

Ying, S. J., and C. C. Chang, 1970: Exploratory model study of tornado-like vortex dynamics. *J. Atmos. Sci.*, **27**, 3–14.